

# Size-, Mass-, and Density-Controlled Preparation of TiO<sub>2</sub> Nanoparticles in a Spherical Coordination Template

Tatsuya Ichijo, Sota Sato, and Makoto Fujita\*

Department of Applied Chemistry, School of Engineering, The University of Tokyo, 7-3-1 Hongo, Bunkyo-ku, Tokyo 113-8656, Japan

**S** Supporting Information

**ABSTRACT:** TiO<sub>2</sub> nanoparticles were prepared with strict control of the size, molecular mass (PDI = 1.02), and mass density by hydrolyzing a precursor, Ti(acac)<sub>2</sub>(biphen), in the presence of a well-defined hollow Pd<sub>12</sub>L<sub>24</sub> spherical endotemplate. The formation of highly monodisperse TiO<sub>2</sub> nanoparticles was confirmed by <sup>1</sup>H NMR spectroscopy, MALDI–TOF mass spectrometry, transmission electron microscopy, and atomic force microscopy. The template was easily removed by treating the sphere with a metal scavenger followed by calcination to give crystalline TiO<sub>2</sub> nanoparticles (2.0 ± 0.2 nm in diameter), which showed photocatalytic activity.

Titanium (TiO<sub>2</sub>)<sup>1</sup> is a well-known photocatalyst with various applications ranging from water splitting to the decomposition of pollutants and use in self-cleaning surfaces.<sup>2</sup> Controlling the size of TiO<sub>2</sub> particles on the nanometer scale, particularly below 3 nm, is an important task in this field because the band gap of TiO<sub>2</sub> nanoparticles is highly sensitive to the size of the nanoparticles because of the quantum size effect.<sup>3,4,6</sup> TiO<sub>2</sub> particles on a nano-to-micrometer scale are normally prepared within micelle templates; however, the sizes of these templates are considerably dispersed.<sup>5</sup> Recently, strict size control of TiO<sub>2</sub> nanoparticles with diameters of ~1 nm was achieved using a dendrimer template,<sup>6</sup> but this method required the tedious synthesis of the template. In this work, we succeeded in the templated synthesis of <3 nm TiO<sub>2</sub> nanoparticles with strict control of the size and molecular mass by using a self-assembled M<sub>12</sub>L<sub>24</sub> spherical complex<sup>7</sup> as a template (Figure 1). Moreover, the mass density of the TiO<sub>2</sub> nanoparticles could also be controlled. Silica nanoparticles were previously synthesized within the same template, but the removal of the template without particle fusion was impossible.<sup>8</sup> In contrast, the coordination shell around the TiO<sub>2</sub> nanoparticles could be removed easily by treating the complex with a metal scavenger followed by calcination. After calcination, the template-free TiO<sub>2</sub> was shown to exist as size-defined crystalline nanoparticles (2.0 ± 0.2 nm in diameter), which were active for the photocatalytic degradation of an organic dye.

Ligand **1** was synthesized according to the reported method<sup>8</sup> and assembled into sphere **2** upon complexation with Pd(II). The sugar pendant of **1** is essential to make the interior of **2** hydrophilic and to trap hydrolyzed TiO<sub>2</sub> precursors therein. Thus, ligand **1** (14 μmol) was treated with Pd(NO<sub>3</sub>)<sub>2</sub> (7.07

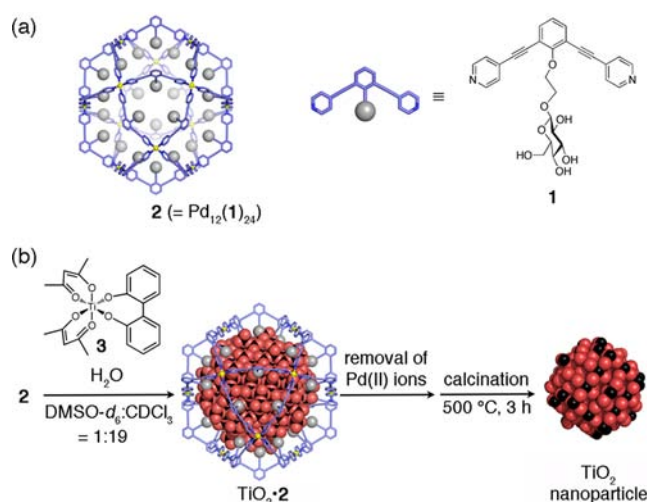


**Figure 1.** (a) Structures of **1** and **2**. Yellow spheres in sphere **2** denote Pd(II) ions. (b) Schematic representation of the synthesis of TiO<sub>2</sub> nanoparticles.

μmol) in dimethyl sulfoxide (DMSO) (0.70 mL) at 50 °C for 2 h to give a DMSO solution of Pd<sub>12</sub>L<sub>24</sub> sphere **2** (0.83 mM). A portion of the DMSO solution (0.15 mL) was diluted with chloroform (2.85 mL) to make the outer environment of sphere **2** hydrophobic.

To this solution, a trace amount of water (0.8 μL) was added, and the most common TiO<sub>2</sub> precursor, Ti(O<sup>i</sup>Pr)<sub>4</sub> (96 equiv), was added in one portion. The trace water content was essential to promote the hydrolysis of the precursor. Under the conditions, however, TiO<sub>2</sub> was formed not within sphere **2** but in the bulk solvent, resulting in the formation of a TiO<sub>2</sub> suspension (Figure S5 in the Supporting Information). Presumably as a result of the high hydrolysis rate of Ti(O<sup>i</sup>Pr)<sub>4</sub>, the condensation reaction proceeded outside sphere **2** before the precursors were trapped in the interior.

This result prompted us to employ other TiO<sub>2</sub> precursors with lower hydrolysis rates. After screening several precursors and condensation conditions, we finally found that the condensation proceeded only within the sphere, without the precipitation of bulk TiO<sub>2</sub>, when Ti(acac)<sub>2</sub>(biphen)<sup>9</sup> (**3**) (acac = acetylacetonate, biphen = 2,2'-biphenoxide) was employed as a precursor with a trace amount of water. The rate of hydrolysis

Received: February 25, 2013

Published: April 22, 2013

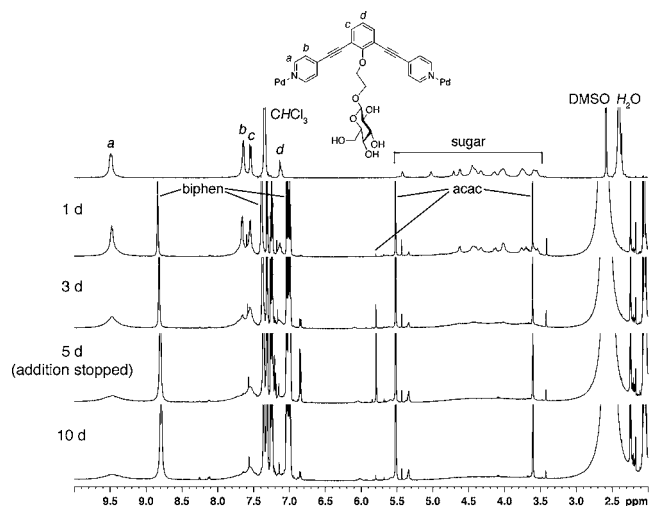


**Figure 2.**  $^1\text{H}$  NMR (500 MHz, 300 K, 19:1  $\text{CDCl}_3/\text{DMSO}-d_6$ ) observation of the synthesis of  $\text{TiO}_2$  nanoparticles within **2**: (top to bottom) before addition of **3** and 1, 3, 5, and 10 days after beginning the addition of **3** at an addition rate of 1.0 equiv/h.

of **3** is much lower than that of  $\text{Ti}(\text{O}^i\text{Pr})_4$  because of the chelation of the biphen and acac ligands on the Ti atom. Experimentally, very slow addition of **3** to the solution of **2** using a syringe pump was important to suppress completely the condensation outside the sphere (Figures S6 and S7). Thus, precursor **3** (108 equiv, dried  $\text{CDCl}_3$  solution) was added via a syringe pump at an addition rate of 1.0 equiv/h to a solution of **2** in 19:1  $\text{CDCl}_3/\text{DMSO}-d_6$ , and the reaction was monitored by  $^1\text{H}$  NMR spectroscopy (Figure 2). The signals from sphere **2** gradually broadened upon addition of precursor **3** and the solution remained transparent, indicating that the  $\text{TiO}_2$  particles formed gradually within spherical complex **2**.

From diffusion-ordered NMR spectroscopy (DOSY) experiments, the diffusion coefficient of sphere **2** was measured before and after condensation of precursor **3** (Figure S9). During the condensation, the diffusion coefficient of **2** was constant at  $D = 2.1 \times 10^{-10} \text{ m}^2 \text{ s}^{-1}$ , showing that the condensation reaction of precursor **3** occurred only within sphere **2** and that no intermolecular cross-linking between spheres occurred. This was supported by atomic force microscopy (AFM) (Figure 3a,b), which clearly showed well-separated particles with a uniform height consistent with the diameter of the framework of **2** (4.6 nm).

The extremely narrow size and molecular mass distributions of the  $\text{TiO}_2$  nanoparticles were revealed by transmission electron microscopy (TEM) and mass spectrometry (MS) measurements, respectively. The TEM images showed highly dispersed nanoparticles with a diameter of  $2.8 \pm 0.2 \text{ nm}$  (Figure 3c,d). The shell framework of **2** was not observed. In the MALDI–TOF MS analysis, the  $\text{Pd}_{12}\text{L}_{24}$  shell framework of **2** was destroyed under the measurement conditions, and the molecular mass of the  $\text{TiO}_2$  nanoparticles was directly observed at  $m/z \sim 10000$  with a polydispersity index close to unity ( $M_w/M_n = 1.017$ ; Figure 3e). The molecular mass remained constant even after 3 months, showing the high stability of the nanoparticles formed in sphere **2**.

The molecular mass and particle size were controlled by changing the amount of precursor: the condensation of 46 to 108 equiv of **3** showed a gradual increase in the molecular mass (6174 to 9972 Da, respectively) while maintaining the narrow

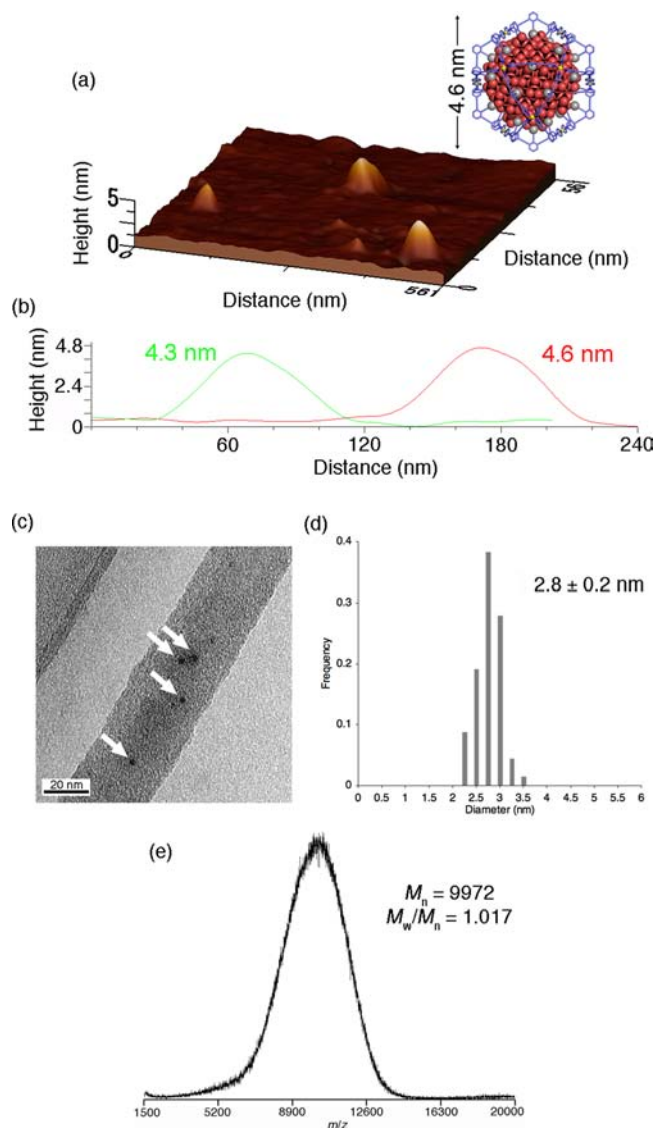


**Figure 3.** (a) AFM image of  $\text{TiO}_2$ :**2** on mica. (b) Height profile of the AFM image of  $\text{TiO}_2$ :**2** from (a). Well-separated particles having heights consistent with the diameter of **2** (4.6 nm) were observed. (c) TEM image of  $\text{TiO}_2$  nanoparticles within **2** (amount of **3** = 108 equiv, addition rate = 1.0 equiv/h). (d) Size distribution determined from TEM images of  $\text{TiO}_2$  nanoparticles within **2**. (e) MALDI–TOF MS spectrum of  $\text{TiO}_2$  nanoparticles ( $M_n = 9972 \text{ Da}$ ;  $M_w/M_n = 1.017$ ) within **2** (amount of **3** = 108 equiv, addition rate = 1.0 equiv/h, matrix = DCTB). Under the conditions, the polycationic shell was broken and only monocharged  $\text{TiO}_2$  nanoparticles were observed.

**Table 1. Characteristic Parameters of  $\text{TiO}_2$  Nanoparticles Synthesized within **2** at Addition Rates of (a) 1.0 and (b) 0.25 equiv/h<sup>a</sup>**

(a) 1.0 equiv/h			(b) 0.25 equiv/h		
precursor (equiv)	$M_n$ of $\text{TiO}_2$ (Da)	diameter (nm)	precursor (equiv)	$M_n$ of $\text{TiO}_2$ (Da)	diameter (nm)
46	6174	$2.2 \pm 0.2$	45	~6300	$1.8 \pm 0.2$
72	7250	$2.4 \pm 0.2$	70	6961	$2.0 \pm 0.2$
93	8297	$2.6 \pm 0.2$	95	8777	$2.1 \pm 0.2$
108	9972	$2.8 \pm 0.2$	107	10386	$2.2 \pm 0.2$

<sup>a</sup> $M_n$  was determined by MALDI–TOF MS and the diameter by TEM.

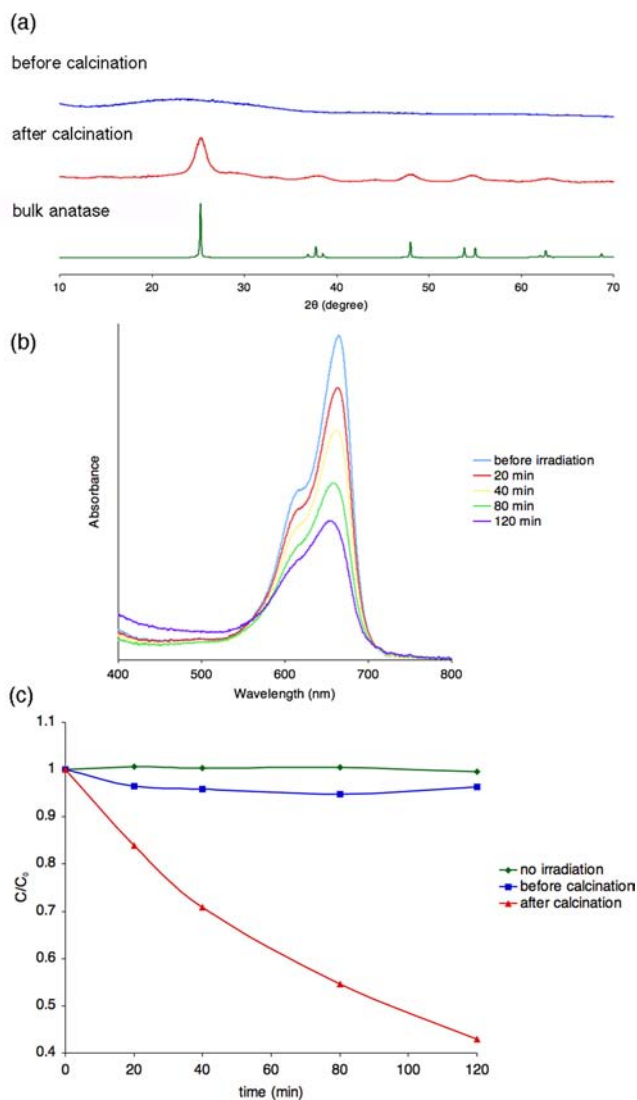


**Figure 4.** (a) PXRD patterns of the template-free TiO<sub>2</sub> nanoparticles before calcination, TiO<sub>2</sub> nanoparticles after calcination at 500 °C for 3 h, and bulk anatase TiO<sub>2</sub> powder as a standard sample. (b) UV–vis absorption spectra monitoring the degradation of methylene blue using TiO<sub>2</sub> nanoparticles after calcination at 500 °C for 3 h. (c) Photodegradation curves for methylene blue.

distribution in particle size (Table 1a). In addition to size and mass, the mass density could also be controlled simply by controlling the addition rate of the precursor. Changing the addition rate from 1.0 to 0.25 equiv/h did not significantly affect the molecular mass of the nanoparticles formed (Table 1b). However, the diameter of those formed at an addition rate of 0.25 equiv/h ( $2.2 \pm 0.2$  nm) was much smaller than that of the ones formed at 1.0 equiv/h ( $2.8 \pm 0.2$  nm), indicating the formation of much denser particles at the lower addition rate. Presumably, slow particle growth in the sphere at the lower addition rate enabled the formation of denser particles.

To evaluate the photocatalytic activity of the obtained TiO<sub>2</sub> nanoparticles, the Pd<sub>12</sub>L<sub>24</sub> shell was removed and crystalline TiO<sub>2</sub> nanoparticles were prepared as follows. TiO<sub>2</sub> nanoparticles synthesized on a preparative scale at the addition rate of 0.55 equiv/h with 91 equiv of precursor 3 were treated with the metal scavenger QuadraPure TU (beads of porous polystyrene functionalized with thiourea moieties)<sup>10</sup> to remove

the Pd(II) ions. Next, the template-free TiO<sub>2</sub> nanoparticles were precipitated by the addition of poor solvents (AcOEt and hexane). TEM observations confirmed the formation of highly dispersed TiO<sub>2</sub> nanoparticles. The diameter of the nanoparticles was determined to be  $2.3 \pm 0.2$  nm. Subsequently, the precipitated powder was calcined at 500 °C for 3 h in air.

Powder X-ray diffraction (PXRD) analysis of the calcined nanoparticles confirmed that the amorphous TiO<sub>2</sub> nanoparticles were dominantly converted to the anatase phase by calcination (Figure 4a). Analysis of TEM images showed that the size of the TiO<sub>2</sub> nanoparticles was slightly reduced from  $2.3 \pm 0.2$  to  $2.0 \pm 0.2$  nm. Thus, the extremely narrow size distribution and the small particle size were maintained without particle fusion even after calcination.

The photocatalytic activity of the calcined anatase TiO<sub>2</sub> nanoparticles for the degradation of methylene blue with a UV lamp (0.286 mW/cm<sup>2</sup>, wavelength: 254 nm) was then investigated.<sup>11</sup> The photodegradation was monitored by UV–vis absorption measurements (Figure 4b), and the methylene blue gradually decomposed under UV irradiation. As control experiments, the degradation was carried out without irradiation or in the presence of the amorphous nanoparticles before calcination. In both cases, the degradation of methylene blue was negligible, demonstrating the photocatalytic activity of the anatase nanoparticles after calcination (Figure 4c).

In summary, we succeeded in controlling the size, mass, and mass density of TiO<sub>2</sub> nanoparticles with an extremely narrow size distribution by using a Pd<sub>12</sub>L<sub>24</sub> spherical complex as an endotemplate. Furthermore, after removal of the Pd(II) ions followed by calcination, crystalline TiO<sub>2</sub> nanoparticles with an extremely narrow size distribution were obtained and subsequently used as a photocatalyst. We note that the precise control of particle size and density in the region below 3 nm is difficult using any other synthetic method and that our method can easily provide high-quality TiO<sub>2</sub> nanoparticle samples in this region in which the quantum size effect can be expressed.

## ■ ASSOCIATED CONTENT

### 📄 Supporting Information

Experiment details and characterization data. This material is available free of charge via the Internet at <http://pubs.acs.org>.

## ■ AUTHOR INFORMATION

### Corresponding Author

mfujita@appchem.t.u-tokyo.ac.jp

### Notes

The authors declare no competing financial interest.

## ■ ACKNOWLEDGMENTS

This research was supported by JST CREST and JSPS KAKENHI (24000009) and also in part by MEXT KAKENHI and Nanonet at the University of Tokyo.

## ■ REFERENCES

- (1) “TiO<sub>2</sub>” is a trivial term for titania that is used throughout the manuscript, even though the exact composition of titania is TiO<sub>x</sub> ( $x > 2.0$ ).
- (2) (a) Fujishima, A.; Honda, K. *Nature* **1972**, *238*, 37. (b) Fujishima, A.; Rao, T. N.; Tryk, D. A. *J. Photochem. Photobiol., C* **2000**, *1*, 1. (c) Chen, X.; Mao, S. S. *Chem. Rev.* **2007**, *107*, 2891. (d) Fujishima, A.; Zhang, X.; Tryk, D. A. *Surf. Sci. Rep.* **2008**, *63*, 515.

- (3) (a) Alivisatos, A. P. *Science* **1996**, *271*, 933. (b) Wang, Y.; Herron, N. J. *J. Phys. Chem.* **1991**, *95*, 525. (c) Roduner, E. *Chem. Soc. Rev.* **2006**, *35*, 583.
- (4) (a) Li, Y. F.; Liu, Z. P. *J. Am. Chem. Soc.* **2011**, *133*, 15743. (b) Serpone, N.; Lawless, D.; Khairutdinov, R. *J. Phys. Chem.* **1995**, *99*, 16646. (c) Anpo, M.; Shima, T.; Kodama, S.; Kubokawa, Y. *J. Phys. Chem.* **1987**, *91*, 4305. (d) Kormann, C.; Bahnemann, D. W.; Hoffmann, M. R. *J. Phys. Chem.* **1988**, *92*, 5196.
- (5) (a) Lin, J.; Lin, Y.; Liu, P.; Meziani, J. M.; Allard, F. L.; Sun, Y. J. *Am. Chem. Soc.* **2002**, *124*, 11514. (b) Spatz, J.; Mössmer, S.; Möller, M.; Kocher, M.; Neher, D.; Wegner, G. *Adv. Mater.* **1998**, *10*, 473. (c) Stathatos, E.; Lianos, P.; Del Monte, F.; Levy, D.; Tsiourvas, D. *Langmuir* **1997**, *13*, 4295.
- (6) Satoh, N.; Nakashima, T.; Kamikura, K.; Yamamoto, K. *Nat. Nanotechnol.* **2008**, *3*, 106.
- (7) (a) Tominaga, M.; Suzuki, K.; Kawano, M.; Kusukawa, T.; Ozeki, T.; Sakamoto, S.; Yamaguchi, K.; Fujita, M. *Angew. Chem., Int. Ed.* **2004**, *43*, 5621. (b) Tominaga, M.; Suzuki, K.; Murase, T.; Fujita, M. *J. Am. Chem. Soc.* **2005**, *127*, 11950. (c) Sato, S.; Iida, J.; Suzuki, K.; Kawano, M.; Ozeki, T.; Fujita, M. *Science* **2006**, *313*, 1273.
- (8) (a) Suzuki, K.; Sato, S.; Fujita, M. *Nat. Chem.* **2010**, *2*, 25. (b) Suzuki, K.; Takao, K.; Sato, S.; Fujita, M. *Angew. Chem., Int. Ed.* **2011**, *50*, 4858.
- (9) Tsotetsi, A. T.; Kuhn, A.; Muller, A.; Conradie, J. *Polyhedron* **2009**, *28*, 209.
- (10) Richardson, J. M.; Jones, C. W. *Adv. Synth. Catal.* **2006**, *348*, 1207.
- (11) Asahi, R.; Morikawa, T.; Ohwaki, T.; Aoki, K.; Taga, Y. *Science* **2001**, *293*, 269.